Application value of Philips Ingenuity TF PET/CT scanner imaging agent FAP in evaluating renal fibrosis

Xueqin Zhao MD,
Wei Fu MD

Department of Nuclear Medicine, Affiliated Hospital of Guilin Medical University, Guilin 541000, Guangxi Zhuang Autonomous Region, China

Keywords: FAP - Philips ingenuity TF PET/CT scanner imaging
- Renal fibrosis
- Glomerular filtration rate (GFR)
- Radiotracer uptake

Corresponding author:
Wei Fu MD,
Department of Nuclear Medicine,
Affiliated Hospital of Guilin Medical University,
Guilin 541000, Guangxi Zhuang Autonomous Region, China
zxq1232024@126.com

Received:
23 October 2024
Accepted revised:
2 January 2025

Abstract

Objective: Chronic kidney disease (CKD) progression is accelerated by renal fibrosis, which causes abnormal extracellular matrix (ECM) accumulation. Non-invasive precision in measuring renal fibrosis is now possible with the help of advanced imaging techniques like magnetic resonance imaging (MRI) and ultrasound elastography. Fluorine-18-fibroblast activation protein (^{18}F-FAP) is a promising Philips ingenuity TF positron emission tomography/computed tomography (PET/CT) scanner imaging target in activated fibroblasts associated with fibrotic disorders. Real-time quantification with FAP-targeted imaging improves kidney fibrosis diagnosis and guides anti-fibrotic therapies. The aim of this study is to develop reliable diagnostic and treatment techniques for renal fibrosis, Philips ingenuity TF PET/CT scanner imaging with FAP is useful. **Materials and Methods:** Positron emission tomography data from 100 patients in our hospital (October 2022-September 2023) was analyzed to see if renal radiotracer uptake correlated with CKD progression. Fluorine-18-FAPI-04 synthesis and Philips ingenuity TF PET/CT scanner imaging were standard. One person determined CKD stage and glomerular filtration rate (GFR) after imaging processing. Imaged renal radiotracer distribution using maximum standardized uptake value (SUVmax) and mean SUV (SUVmean). The study sought to improve renal radiotracer dispersion estimation for CKD assessment. **Results:** The study reveals a complex relationship between GFR and radiotracer uptake in kidneys. At lower GFR, substantial uptake is seen, but a GFR of 15mL/min/1.73m^2 shows a drop to zero. Higher GFR generally correlate with increased uptake, peaking at GFR of 75 and 90mL/min/1.73m^2. Yet, at GFR of 115 and 120mL/min/1.73m^2, there is a reduction in radiotracer uptake, suggesting a nuanced association with renal function. Varied kidney SUVmax and SUVmean were significant for ^{18}F-FAPI C ($P<0.001$), while baseline SUV readings were not significant. Fluorine-18-L-dihydroxyphenylalanine (^{18}F-DOPA) and gallium-68 (^{68}Ga) ^{18}F-prostate specific membrane antigen (PSMA) had significant kidney SUVmax values ($P=0.05$). Results suggest diverse absorption patterns for different radiotracers in kidneys and tissues. **Conclusion:** Fluorine-18-FAPI is a promising noninvasive approach for evaluating and quantifying CKD grades. Its excellent CKD severity correlation and renal insights make it a transformative diagnostic tool.

Hell J Nucl Med 2025; 28(1): 28-35 *Epub ahead of print: 7 April 2025* *Published online: 30 April 2025*

Introduction

Renal fibrosis, a prevalent pathological phenomenon across diverse kidney diseases, poses a substantial threat by instigating progressive kidney deterioration, ultimately culminating in renal failure. This intricate process manifests through the aberrant accumulation of extracellular matrix (ECM) proteins, notably collagen, within the kidney tissue. The consequential ECM deposition disrupts the inherent architecture and functionality of the kidney, precipitating organ failure as a dire consequence. Renal fibrosis exhibits its deleterious impact on various kidney compartments, encompassing the glomeruli, tubulointerstitium, and vasculature. The intricate web of cellular and molecular mechanisms propelling this fibrotic cascade involves the activation of fibroblasts, epithelial-to-mesenchymal transition, and the influence of profibrotic factors, prominently exemplified by transforming growth factor-beta (TGF-beta) [1-3]. The pathogenesis of renal fibrosisis schematically presented below (Figure 1).

It's imperative to acknowledge its significance in the context of chronic kidney disease (CKD). Chronic kidney disease, a global health concern, boasts an estimated prevalence of 13.4%, underscoring its substantial impact on global morbidity and mortality. Within the realm of CKD, renal fibrosis emerges as a pivotal player, contributing significantly to disease progression. The insidious accumulation of extracellular matrix in the kidney characterises renal fibrosis, imparting a formidable challenge in the clinical landscape and amplifying the complexity of managing CKD [4, 5].

The evaluation of renal fibrosis holds paramount significance as it furnishes crucial in-

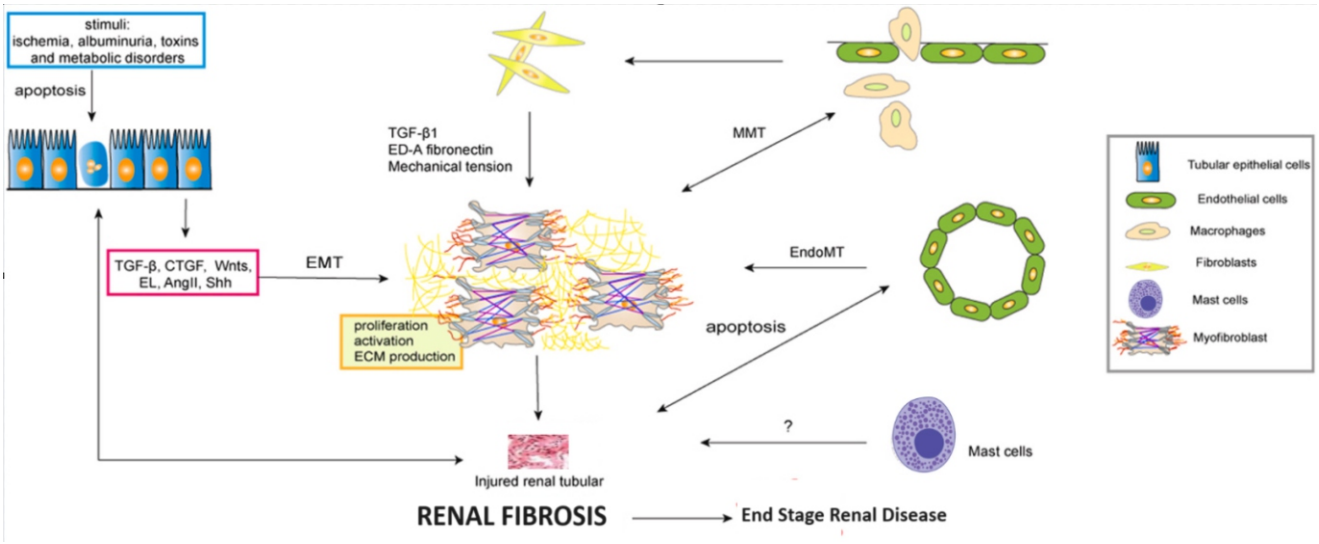

Figure 1. The pathogenesis of renal fibrosis.

sights into the progression and prognostication of diverse kidney disorders, encompassing CKD and renal cell carcinoma (RCC). Serving as a hallmark of kidney damage, the undue accumulation of extracellular matrix precipitates fibrosis, posing a substantial threat to renal function. The assessment of renal fibrosis emerges as a linchpin in gauging the gravity of kidney ailments, steering treatment strategies, and forecasting patient outcomes. Employing a repertoire of techniques, including histopathology, magnetic resonance imaging (MRI), shear wave elastography (SWE), and diffusion-weighted MRI, facilitates a comprehensive evaluation of fibrosis. These methodologies not only unveil the extent and distribution of fibrotic changes but also pave the way for enhanced management and vigilant monitoring of kidney diseases [6-14].

The precision of renal fibrosis assessment methods is paramount due to the strong correlation between renal fibrosis and CKD. As a progressive and irreversible process culminating in the loss of kidney function, renal fibrosis necessitates accurate evaluation. Traditional approaches like renal biopsy, although effective, are invasive and susceptible to sampling errors. The advent of advanced imaging techniques, including MRI and ultrasound elastography, presents a promising avenue for noninvasive renal fibrosis assessment. These techniques excel in detecting alterations in tissue stiffness, water molecule diffusion, and renal tissue oxygenation and perfusion, offering objective and quantitative indices of fibrosis. The accurate evaluation facilitated by advanced imaging not only aids in the diagnosis and prognosis of CKD but also enhances the overall management of affected patients [15-22].

Positron emission tomography/computed tomography (Philips ingenuity TF PET/CT scanner) stands as a formidable imaging tool amalgamating functional and anatomical insights, delving into intricate tissue changes. Harnessing a radioactive tracer like fluorine-18-2-fluoro-2-deoxy-D-glucose (^{18}F-FDG), PET captures the metabolic vigor of cells. The emitted positrons are keenly detected, crafting nuanced functional images. On the flip side, CT employs X-rays for finely detailed anatomical portraits. The marriage of PET and CT in Philips ingenuity TF PET/CT scanner amplifies diagnostic precision, deftly pinpointing metabolic activity to specific anatomical realms. This synergy proves transformative across diverse domains, from oncology and cardiology to neurology, elevating diagnostic acumen and refining treatment stratagems [23].

Fluorine-18-fibroblast activation protein (^{18}F-FAP) takes center stage as a membrane-bound serine protease, wielding prominence on the battleground of activated fibroblasts. These fibroblasts, donned as myofibroblasts, orchestrate the unfolding drama of fibrosis, marked by the unruly buildup of extracellular matrix (ECM) in tissues. Fluorine-18-FAP, a discerning marker adorning activated fibroblasts, partakes in a ballet of activities crucial to fibrosis-unleashing fibroblast activation, choreographing ECM production, and directing the symphony of tissue remodeling. Intriguingly, studies illuminate ^{18}F-FAP as a linchpin; targeting it emerges as a promising avenue to temper fibrosis, orchestrating a dance that may alleviate tissue dysfunction. Consequently, FAP emerges as a beacon on the therapeutic horizon, offering a potential bull's eye for interventions combating the intricacies of fibrotic diseases [24-30].

Fluorine-18-FAP, a membrane-anchored enzyme prevalent in activated fibroblasts, particularly cancer-associated fibroblasts (CAF), emerges as a promising protagonist for imaging and therapeutic endeavors in diverse ailments, including renal fibrosis. The rationale underlying ^{18}F-FAP's role as a Philips ingenuity TF PET/CT scanner imaging agent for assessing renal fibrosis lies in its specificity to activated fibroblasts, pivotal in extracellular matrix deposition and kidney tissue scarring. This cutting-edge imaging technique, distinct from conventional methods, offers non-invasive, real-time quantification of fibroblast activation, providing a sensitive, specific lens to pinpoint and characterize renal fibrosis lesions. Additionally, ^{18}F-FAP-specific Philips ingenuity TF PET/CT scanner imaging holds the potential to steer targeted therapies, identifying candidates poised to benefit from anti-fibrotic interventions [31].

Materials and Methods

Research design

This retrospective study examined PET data from 100 patients who were admitted in our hospital's Nuclear Medicine departments from October 2022 to September 2023. The mean age was 69.2 years, 51 were male and 49 were female. Radiotracer production and labelling procedures had previously been described, and standard procedures were followed for Philips ingenuity TF PET/CT scanner imaging. Hospital databases provided laboratory values, patient history, and Philips ingenuity TF PET/CT scanner imaging. Recent Philips ingenuity TF PET/CT scanner scans employing the prescribed radiotracers were necessary for inclusion. Still, nephrectomy, ureteral system obstruction, or inability to produce imaging or laboratory values were excluded. The purpose of this investigation was to examine the relationship between renal uptake of radiotracers and the progression of CKD. The CKD stage and GFR were determined after image analysis, which was performed by a solitary experienced observer to guarantee impartial assessments. With this all-encompassing approach, we hoped to learn more about how various radiotracers were distributed throughout the kidneys and what that would mean for assessing CKD.

Imaging and radiotracer synthesis and data analysis

Using a Siemens Biograph mCT Flow scanner, Philips ingenuity TF Philips ingenuity TF PET/CT scanner scanner of ^{18}F-FAPI-42 was performed in Heidelberg according to the method described by experts who were responsible for examining and labelling FAPI tracers by the guidelines of our hospital. The imaging agent is produced by GE PET trace 16.5 MeV medical cyclotron, the pH value is about 7.0, and the radiographic chemical purity is >95%. The injected activity for ^{18}F-FAPI exams was between 113 and 340MBq, and PET scans began 1h after injection, moving from the head to the toes. At the university medical centre, we injected 2MBq/kg of body weight of patients receiving ^{18}F-DOPA or ^{18}F-PSMA and then checked on them after 60 minutes. A Philips ingenuity TF PET/CT scanner scanner, namely a Philips Gemini TF 16, was used for the imaging. Fluorine-18-L-dihydroxyphenylalanine (DOPA) and ^{18}F-prostate specific membrane antigen (PSMA) required different imaging orientations, with the arms lifted to minimize artefacts. A low-dose unenhanced CT from the base of the head to the upper thigh was done for attenuation correction. The ^{18}F-PSMA-HBED-CC tracer was manufactured in-house using a described procedure. For the synthesis of ^{18}F-DOPA, the Scintomics cassette-based synthesis module GRP-3 V was used. Clinical Philips ingenuity TF PET/CT scanner imaging and data analysis involve individual review by a single expert observer in nuclear medicine to reduce inter-observer variation. To reduce the possibility of error, patients' images were analyzed before their CKD stages and GFR were determined. The PET scans were analyzed to observe where the radiotracer was being taken up. Positron emission tomography and low-dose CT images were combined to provide anatomical clarity. Maximum standardized uptake value (SUVmax) and mean SUV (SUVmean) were used to measure the uptake of all three radiotracers in the kidney in distinct regions of the parenchyma also known as the superior, middle, and inferior renal cortex. Background activity was assessed by measuring blood flow in the abdominal aorta at the level of the renal arteries, as well as in the lung parenchyma, myocardium, and gluteal muscles. Methods were developed to assess the possible consequences of radiotracer uptake in renal tissues for the assessment of chronic kidney disease.

Statistical analysis

The data analysis was conducted using SPSS 22.0 software (SPSS Inc., Chicago, IL). The normality tests have indicated that a normal distribution is present in all of the groups. The statistical techniques of linear regression and one-way analysis of variance (ANOVA) were utilized to evaluate the relationship between GFR and SUVmax or SUVmean. In order to conduct a comparison of age structures among different patient groups, a statistical analysis known as Student's t-test was utilized.

Results

Table 1 shows the percentage of patients who fall into each CKD group for each radiotracer. GFR >90 (9), 60-89 (4), 30-59 (8), and 30 (3) were the most common ranges in the ^{18}F-FAPI-42 cohort. The highest number of subjects in the 60-89 GFR range was ^{18}F-PSMA (27), the highest number of subjects in the >90 GFR range were ^{18}F-DOPA (8), and the totals for ^{18}F-FAPI-42 and ^{18}F-DOPA were very close (24 and 26). This distribution provides insights into the incidence of CKD stages within each radiotracer group, vital for identifying potential associations between renal function and radiotracer performance.

Figure 2 presents the uptake of the ^{18}F-FAPI-42 radiotracer in the kidneys across different levels of GFR, measured in milliliters per minute per 1.73 square meters (mL/min/1.73m^2). The two parameters analyzed are the SUV representing the SUVmax and SUVmean radiotracer uptake in the kidneys. As GFR decreases, indicating declining kidney function, there is a noticeable trend in the SUVmax and SUVmean values. At a GFR of 0 mL/min/1.73m^2, the SUVmax is 5, and SUVmean is 3.5, indicating a moderate radiotracer uptake. As GFR increases to 15mL/min/1.73m^2, there is a slight increase in both SUVmax (5.6) and SUVmean (3.8). However, as GFR further increases to 60mL/min/1.73m^2, the SUVmax drops to 2.9, and SUVmean decreases to 1.8, suggesting a reduction in radiotracer uptake with declining kidney function. The lowest values are observed at a GFR of 75mL/min/1.73m^2, with SUVmax at 1.9 and SUVmean at 1, indicating a significant decrease in radiotracer accumulation. Subsequently, as GFR fluctuates around 90mL/min/1.73m^2, there is a modest increase in both SUVmax (2.3) and SUVmean (1.1), suggesting a potential recovery in radiotracer uptake. At higher GFR values of 100, 115, and 120mL/min/1.73m^2, there is a general upward trend in both SUVmax and SUVmean, indicating increased radiotracer uptake as kidney function improves. The observed variations in SUV values across different GFR levels

Table 1. *Number of patients in each CKD category across radiotracer groups.*

GFR	^{18}F-FAPI-42	^{18}F-PSMA	^{18}F-DOPA	Total
>90	9	10	8	27
60-89	4	27	8	39
30-59	8	7	6	21
<30	3	6	2	11
Total	24	50	26	100

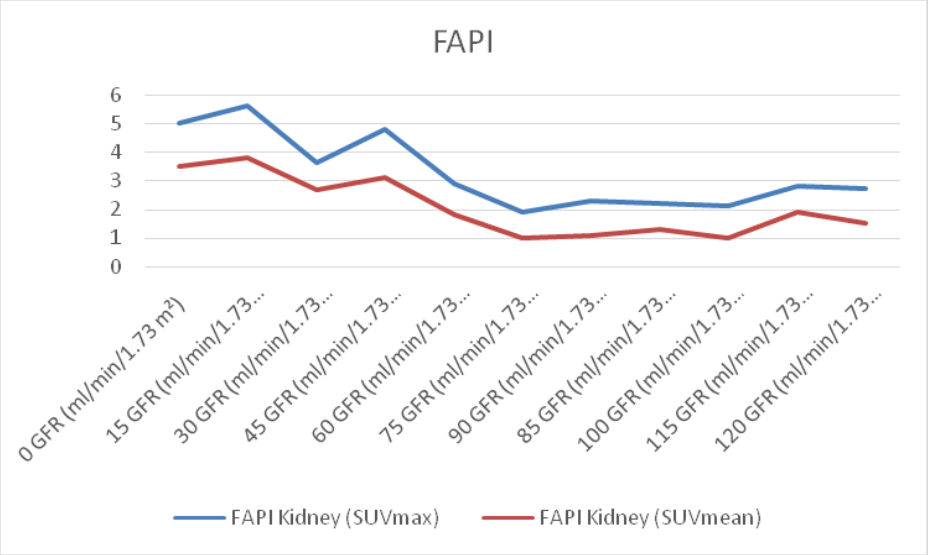

Figure 1. Comparison of linear regression analyses of the correlation between kidney SUVmean and SUVmax with that of GFR for ^{18}F-FAPI-42 radiotracer.

provide valuable insights into the radiotracer's performance and its potential utility in assessing renal function in clinical settings. Interpretation of these findings should consider the specific context of the imaging study and relevant clinical information.

Figure 3 presents data on the uptake of the ^{18}F-DOPA radiotracer in the kidneys across various levels of glomerular filtration rate (GFR), measured in milliliters per minute per 1.73 square meters (mL/min/1.73m^2). The two parameters analyzed are the SUV representing the SUVmax and SUVmean radiotracer uptake in the kidneys. At a GFR of 0mL/min/1.73m^2, both SUVmax and SUVmean are relatively high at 11.1 and 6.3, respectively, indicating a substantial radiotracer uptake. Interestingly, at a GFR of 15mL/min/1.73m^2, the SUV values drop to zero, suggesting a lack of radiotracer uptake in the kidneys at this specific level of renal function.

As GFR increases from 30 to 120mL/min/1.73m^2, there is variability in the SUVmax and SUVmean values. Generally, there is a fluctuating pattern in both parameters, with higher GFR values associated with increased radiotracer uptake. Notably, at GFR of 90 and 100mL/min/1.73m^2, there is a notable increase in both SUVmax (13.1 and 9.9) and SUVmean (7.2 and 5.9), indicating enhanced radiotracer accumulation as kidney function improves. However, at GFR of 115 and 120mL/min/1.73m^2, there is a decrease in both SUVmax (8.2 and 5.8) and SUVmean (5.9 and 3.9), suggesting a potential reduction in radiotracer uptake at these higher levels of renal function.

Figure 4 depicts data on the uptake of the PSMA radiotracer in the kidneys across different levels of GFR, measured in milliliters per minute per 1.73 square meters (mL/min/1.73m^2). The two parameters analyzed are the SUV representing the SUVmax and SUVmean radiotracer uptake in the kidneys. At a GFR of 0mL/min/1.73m^2, both SUVmax and SUVmean are notably high at 21 and 8, respectively, indicating substantial radiotracer uptake in the kidneys. As GFR decreases to 15mL/min/1.73m^2, both SUV values drop significantly to 2, suggesting a considerable reduction in radiotracer accumulation at this level of impaired renal function. With increasing GFR from 30 to 120mL/min/1.73m^2, there is a general trend of rising SUVmax and SUVmean values. Higher GFR values, such as those at 60, 75, and 90mL/min/1.73m^2, are associated with elevated SUVmax and SUVmean, indicating increased radiotracer uptake in the

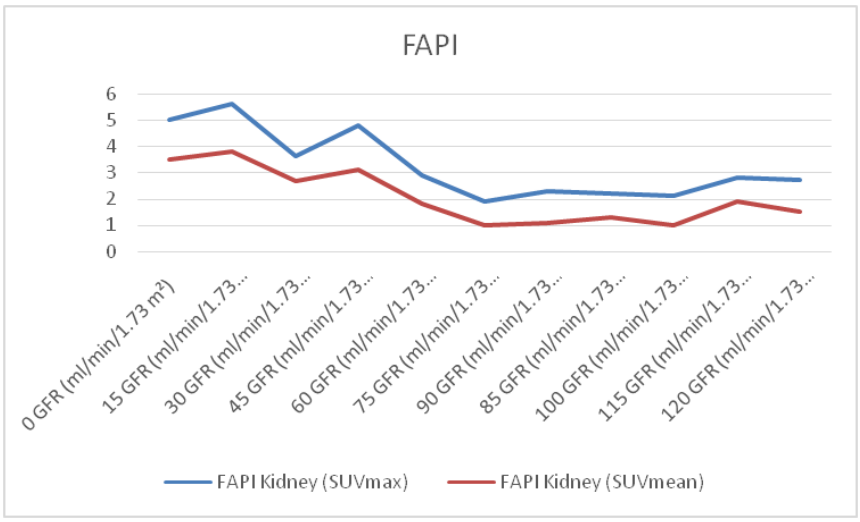

Figure 2. Comparison of linear regression analyses of the correlation between kidney SUVmean and SUVmax with that of GFR for ^{18}F-FAPI-42 radiotracer.

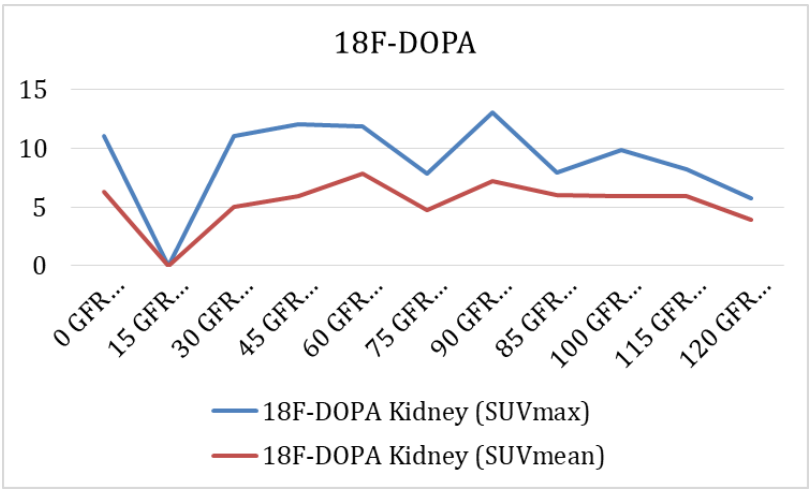

Figure 3. Comparison of linear regression analyses of the correlation between kidney SUVmean and SUVmax with that of GFR for ^{18}F-DOPA radiotracer.

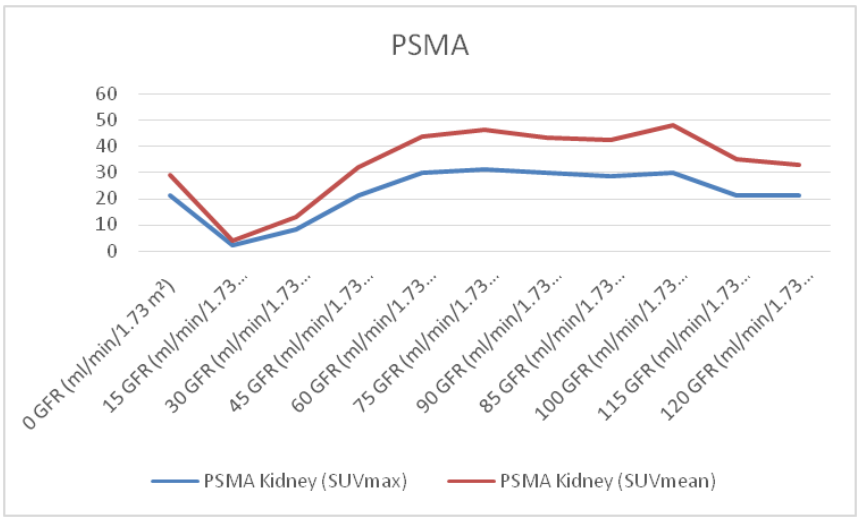

Figure 4. Comparison of linear regression analyses of the correlation between kidney SUVmean and SUVmax with that of GFR for ^{18}F-PSMA radiotracer.

kidneys. Notably, at GFR of 75 and 90mL/min/1.73m^2, both SUVmax and SUVmean peak at values over 30, suggesting a robust radiotracer accumulation as kidney function improves.

However, at GFR of 115 and 120mL/min/1.73m^2, there is a reduction in both SUVmax (21) and SUVmean (12), indicating a potential decrease in radiotracer uptake at these higher levels of renal function.

Table 2 displays the outcomes of comparing the SUVmax and SUVmean values for ^{18}F-FAPI, ^{18}F-DOPA, and ^{18}F-PSMA. Significant variations in kidney SUVmax and SUVmean for ^{18}F-FAPI and ^{18}F-DOPA were found (P<0.001). But the baseline SUV readings showed no statistical significance. The SUVmax values for ^{18}F-DOPA and ^{18}F-PSMA were both statistically significant for the kidney (P=0.05) and for the background (P=0.531 and P=0.003, respectively). These results imply that the kidney and other tissues show varied absorption patterns for various radiotracers.

Table 2. *ANOVA findings for SUVmax and SUVmean evaluation for radiotracer*

Analysis Parameter	df	P-value
^{18}F-FAPI		
SUVmax kidney	1, 15	<0.001
SUVmean kidney	1, 20	<0.001
SUVmean background	1, 18	0.231
SUVmax background	1.20	0.211
^{18}F-DOPA		
SUV max kidney	1,27	0.05
SUV mean kidney	1,24	0.259
SUVmean background	1,23	0.101
SUV max back- ground	1,18	
^{18}F-PSMA		
SUV max kidney	1,25	0.531
SUV max background	1,27	0.003
SUV mean kidney	1, 19	0.002
SUV mean background	1,20	0.003

Discussion

Research by Solano-Iturri et al. (2020) exploring the role of ^{18}F-FAP in renal fibrosis has delved into its implications for chronic kidney disease. Renal fibrosis, marked by the abnormal accumulation of extracellular matrix proteins in the kidney, is a common facet of chronic kidney disease. Notably, studies have scrutinized FAP expression in CAF within renal tumors, particularly in the context of RCC [30, 31]. The intricate study involving 128 patients with renal tumors identified FAP expression in CAF at the tumor center and infiltrating front, notably in clear cell renal cell carcinomas (CCRCC), papillary renal cell carcinomas (PRCC), and chromophobe renal cell carcinomas (ChRCC), but not in benign tumors like renal oncocytoma (RO) [28-32]. The research unveiled a significant correlation between high FAP expression, low levels of soluble isoform sFAP, and adverse tumor characteristics, such as size, grade, and stage. These findings underscore the potential utility of FAP as a biomarker for CCRCC progression, offering insights into its relevance for differential diagnosis among renal tumor subtypes [32].

The clinical experience informs this report's discussion of how CT and MRI staging, tumour size, number, depth, histological grading, and newly developed somatostatin receptor tracers could help determine whether a tumour is benign or malignant, preventing underestimation or overtreatment of rare neoplasms. In numerous recent investigations, SST PET has outperformed scintigraphy in diagnosis.

Lay et al.'s comprehensive review (2019) delves into FAP, accentuating its diagnostic and pathological significance, particularly in liver fibrosis, where FAP plays crucial roles in tissue remodeling and repair. As a member of the dipeptidyl peptidase IV gene family, alongside DPP4, 8, and 9, FAP stands out with its dual functionality as both a dipeptidyl peptidase and endopeptidase. While minimally expressed in healthy tissues, FAP's surge in pathological conditions, especially in areas undergoing tissue remodeling, positions it as a potential biomarker and an enticing target for drug intervention [33]. Comparison of FAPI radiotracer uptake in the kidneys shows a complex connection with GFR. Lower GFR reduce SUVmax and SUVmean, indicating radiotracer buildup and kidney decline. Recovery is possible at GFRs about 90mL/min/1.73m^2, as shown by slight SUV rises. Maximum SUV and SUVmean increase as GFR improves, suggesting radiotracer uptake. These data show the radiotracer's renal function sensitivity, which aids clinical evaluations. A complete comprehension of these dynamic interactions requires careful interpretation in the clinical setting.

Fitzgerald et al.'s (2020) review delves deep into the intricate biology of FAP, shedding light on its involvement not only in oncologic but also non-oncologic diseases. Operating as a versatile actor, FAP engages in processes like extracellular matrix remodeling, intracellular signaling regulation, angiogenesis, epithelial-to-mesenchymal transition, and immunosuppression [32, 33]. Predominantly expressed in pathological conditions like fibrosis, arthritis, and cancer, FAP's type-II transmembrane serine protease nature is uniquely confined to these scenarios. Its elevation, especially in various cancer types, aligns with unfavorable clinical outcomes, yet the pre-

cise biological mechanisms driving these observations remain elusive [34].

The distribution of CKD stages among radiotracers varies. Totals for ^{18}F-FAPI-42 and ^{18}F-DOPA imply similar patient characteristics. With the highest participants in the 60-89 GFR range, ^{18}F-PSMA suggests renal function differences across radiotracers. Understanding these relationships helps improve imaging procedures and radiotracer selection depending on kidney characteristics.

Primary PCa tumours had a positive connection between PSA/GS and ^{18}F-PSMA-1007 uptake. Overall, ^{18}F-PSMA-1007 uptake increased with tumour aggressiveness. High-risk PCa patients had considerably greater SUVmax of prostatic tumour than intermediate-risk individuals. Similar to other PSMA-targeted PET radiopharmaceuticals, ^{18}F-PSMA-1007 has physiological uptake in liver, spleen, salivary glands, lacrimal glands, small intestine, pancreas, and kidneys, but reduced urinary clearance (enabling excellent prostate assessment) and increased hepatobiliary clearance. Fluorine-18-PSMA-1007 injection frequently improves tumor-to-background ratios 2-3h later.

In a study led by Zhou et al. (2021), the diagnostic prowess of a novel PET radiotracer targeting FAP in renal fibrosis was scrutinized. This research unearthed that PET imaging employing FAP exhibited remarkable sensitivity and specificity, outshining the gold standard renal puncture examination. The findings posit Philips ingenuity TF PET/CT scanner imaging with FAP, specifically utilizing [^{68}Ga] ^{18}F-FAPI-04, as a promising non-invasive avenue for the early detection and assessment of renal fibrosis-a critical pathological state in chronic kidney disease progression. The study encompassed a cohort undergoing renal puncture followed by ^{68}Ga-FAPI-04 Philips ingenuity TF PET/CT scanner imaging, with subsequent immunochemistry examinations to validate the results. The [^{68}Ga] ^{18}F-FAPI-04 Philips ingenuity TF PET/CT scanner outcomes showcased heightened radiotracer uptake in almost all patients, with the SUVmax escalating with the severity of fibrosis-3.92±1.50 for mild, 5.98±1.6 for moderate, and 7.67±2.23 for severe cases [35].

Fibroblast activation protein-α emerges as a key player in fibrotic conditions, particularly in renal fibrosis-the ultimate pathological process in chronic kidney disease affecting over 10% of the global population. Renal fibrosis involves excessive extracellular matrix deposition, disrupting functional parenchyma and leading to organ failure. This review delineates the distinct manifestations, cellular origins, and crucial processes in each renal compartment affected by fibrosis-glomerulosclerosis in glomeruli, interstitial fibrosis in tubulointerstitium, and arteriosclerosis/perivascular fibrosis in vasculature [36, 37].

Analyzing thirty studies encompassing 1170 patients, the meta-analysis by Chang et al. (2023) revealed that FAP demonstrated robust potential as a radiotracer in oncology, showcasing relative risks of 1.06 to 3.00-fold per patient and per lesion for primary tumors, recurrent tumors, lymph node metastasis, and distant metastasis. Notably, FAP outperformed ^{18}F-FDG in intensity for various cancers, with pancreatic cancer exhibiting the highest uptake. Fibroblast activation protein exhibited superior sensitivity, diagnostic odds ratio, and summary receiver operating characteristic curve compared to ^{18}F-FDG in detecting primary tumors, lymph node metastasis, and distant metastasis. Despite outstanding sensitivity, FAP tracers for primary tumors showed low specificity, particularly in urological system cancer, emphasizing the need for careful consideration in clinical applications. The distinction in detecting lymph node metastasis between FAP and ^{18}F-FDG remains uncertain in sarcoma cases [38].

Fluorine-18-FAPI-42 is promising for tumour staging before therapy. It detects HCC and non-HCC cancer with ^{18}F-FDG non-avidity and great sensitivity. New cancer imaging tracer ^{18}F-FAPI-42 targets FAP. Fluorine-18-FAPI-42 was used for PET/CT imaging of NSCLC.

The potential of FAP-specific Philips ingenuity TF PET/CT scanner imaging to identify individuals with activated fibroblasts, signaling fibrosis presence, holds promise for selecting candidates benefiting from anti-fibrotic treatments in renal fibrosis. However, further research is crucial to establish the efficacy of FAP-specific Philips ingenuity TF PET/CT scanner imaging in guiding targeted therapies for renal fibrosis, contributing to personalized and effective interventions. Fibroblast activation protein is specifically expressed in activated fibroblasts, and FAP-inhibitor (^{18}F-FAPI-42) PET imaging offers insights into incipient fibrosis. Current studies on ^{18}F-FAPI-42 imaging in cardiovascular diseases highlight its value in early detection, risk stratification, response evaluation, and predicting left ventricular function evolution, emphasizing the need for larger, multicenter studies for comprehensive validation and broader applications [39].

In conclusion, ^{18}F-FAPI-42 is a promising non-invasive method for assessing and quantifying CKD grades. Compared to [^{68}Ga] ^{18}F-DOPA or [^{68}Ga] ^{18}F-PSMA, ^{18}F-FAPI-42 better correlates with CKD severity. The unique capacity of ^{18}F-FAPI-42 to deliver renal function insights is a helpful diagnostic tool for clinicians. This radiotracer could transform CKD evaluation by providing a more detailed view of disease development. The absence of connection with [^{68}Ga] ^{18}F-DOPA or [^{68}Ga] ^{18}F-PSMA uptake highlights [^{68}Ga] ^{18}F-FAPI's specificity and sensitivity in detecting renal problems. As nuclear medicine research improves, [^{68}Ga] ^{18}F-FAPI remains a potential method for noninvasive, precise CKD characterization, enabling better patient care and management methods.

Bibliography

1. Djudjaj S, Boor P. Cellular and molecular mechanisms of kidney fibrosis. *Mol Aspects Med* 2019; 65: 16-36.
2. Chatziantoniou C, Dussaule JC. Insights into the mechanisms of renal fibrosis: is it possible to achieve regression? *Am J Physiol Renal Physiol* 2005; 289(2): F227-34.
3. Lee SY, Kim SI, Choi ME. Therapeutic targets for treating fibrotic kidney diseases. *Transl Res* 2015; 165(4): 512-30.
4. Lv JC, Zhang LX. Prevalence and Disease Burden of Chronic Kidney Disease. *Adv Exp Med Biol* 2019; 1165: 3-15.
5. Wang C, Li SW, Zhong X et al. An update on renal fibrosis: from mechanisms to therapeutic strategies with a focus on extracellular vesicles. *Kidney Res Clin Pract* 2023; 42(2): 174-87.
6. Qin C, Yin H, Liu H et al. The Significance of Fibrosis Quantification as a Marker in Assessing Pseudo-Capsule Status and Clear Cell Renal Cell Carcinoma Prognosis. *Diagnostics (Basel)* 2020; 10(11): 895.

7. Zhao J, Wang ZJ, Liu M et al. Assessment of renal fibrosis in chronic kidney disease using diffusion-weighted MRI. *Clin Radiol* 2014; 69(11): 1117-22.
8. Berchtold L, Friedli I, Vallée JP et al. Diagnosis and assessment of renal fibrosis: the state of the art. *Swiss Med Wkly* 2017; 147: w14442.
9. Zhang J, Yu Y, Liu X et al. Evaluation of Renal Fibrosis by Mapping Histology and Magnetic Resonance Imaging. *Kidney Dis (Basel) 202*1; 7(2): 131-42.
10. Farris AB, Alpers CE. What is the best way to measure renal fibrosis?: A pathologist's perspective. *Kidney Int Suppl* (2011) 2014; 4(1): 9-15.
11. Chen Z, Ying TC, Chen J et al. Assessment of Renal Fibrosis in Patients With Chronic Kidney Disease Using Shear Wave Elastography and Clinical Features: A Random Forest Approach. *Ultrasound Med Biol* 2023; 49(7): 1665-71.
12. Güven AT, Idilman IS, Cebrayilov C et al. Evaluation of renal fibrosis in various causes of glomerulonephritis by MR elastography: a clinicopathologic comparative analysis. *Abdom Radiol (NY)* 2022; 47(1): 288-96.
13. Chen Z, Chen J, Chen H, Su Z. Evaluation of renal fibrosis in patients with chronic kidney disease by shear wave elastography: a comparative analysis with pathological findings. *Abdom Radiol (NY)* 2022; 47(2): 738-45.
14. Nassar MK, Khedr D, Abu-Elfadl HG et al. Diffusion Tensor Imaging in early prediction of renal fibrosis in patients with renal disease: Functional and histopathological correlations. *Int J Clin Pract* 2021; 75(4): e13918.
15. Jiang B, Liu F, Fu H, Mao J. Advances in imaging techniques to assess kidney fibrosis. *Ren Fail* 2023; 45(1): 2171887.
16. Srivastava A, Tomar B, Prajapati S et al. Advanced non-invasive diagnostic techniques for visualization and estimation of kidney fibrosis. *Drug Discov Today* 2021; 26(8): 2053-63.
17. Jiang K, Ferguson CM, Lerman LO. Noninvasive assessment of renal fibrosis by magnetic resonance imaging and ultrasound techniques. *Transl Res* 2019; 209: 105-20.
18. Alnazer I, Bourdon P, Urruty T et al. Recent advances in medical image processing for the evaluation of chronic kidney disease. *Med Image Anal* 2021; 69: 101960.
19. Hysi E, He X, Fadhel MN et al. Photoacoustic imaging of kidney fibrosis for assessing pretransplant organ quality. *JCI Insight* 2020; 5(10): e136995.
20. Thurman J, Gueler F. Recent advances in renal imaging. *F1000Res* 2018; 7: F1000 Faculty Rev-1867.
21. Meola M, Samoni S, Petrucci I. Imaging in Chronic Kidney Disease. *Contrib Nephrol* 2016; 188: 69-80.
22. Leung G, Kirpalani A, Szeto SG et al. Could MRI Be Used To Image Kidney Fibrosis? A Review of Recent Advances and Remaining Barriers. *Clin J Am Soc Nephrol* 2017; 12(6): 1019-28.
23. Kapoor V, McCook BM, Torok FS. An introduction to PET-CT imaging. *Radiographics* 2004; 24(2): 523-43.
24. Yang AT, Kim YO, Yan XZ et al. Fibroblast Activation Protein Activates Macrophages and Promotes Parenchymal Liver Inflammation and Fibrosis. *Cell Mol Gastroenterol Hepatol* 2023; 15(4): 841-67.
25. Xing C, Bao L, Li W, Fan H. Progress on role of ion channels of cardiac fibroblasts in fibrosis. *Front Physiol* 2023; 14: 1138306.
26. Hohn J, Tan W, Carver A et al. Roles of Exosomes in Cardiac Fibroblast Activation and Fibrosis. *Cells* 2021; 10(11): 2933.
27. Nicolini G, Balzan S, Forini F. Activated fibroblasts in cardiac and cancer fibrosis: An overview of analogies and new potential therapeutic options. *Life Sci* 2023; 321: 121575.
28. Cui Y, Wang Y, Wang S et al. Highlighting Fibroblasts Activation in Fibrosis: The State-of-The-Art Fibroblast Activation Protein Inhibitor PET Imaging in Cardiovascular Diseases. *J Clin Med* 2023; 12(18): 6033.
29. Geng Y, Li L, Yan J et al. PEAR1 regulates expansion of activated fibroblasts and deposition of extracellular matrix in pulmonary fibrosis. *Nat Commun* 2022; 13(1): 7114.
30. Wang QR, Liu SS, Min JL et al. CCL17 drives fibroblast activation in the progression of pulmonary fibrosis by enhancing the TGF-β/Smad signaling. *Biochem Pharmacol* 2023; 210: 115475.
31. Lindner T, Loktev A, Giesel F et al. Targeting of activated fibroblasts for imaging and therapy. *EJNMMI Radiopharm Chem* 2019; 4(1): 16.
32. Solano-Iturri JD, Errarte P, Etxezarraga MC et al. Altered Tissue and Plasma Levels of Fibroblast Activation Protein-α (FAP) in Renal Tumours. *Cancers (Basel)* 2020; 12(11): 3393.
33. Lay AJ, Zhang HE, McCaughan GW, Gorrell MD. Fibroblast activation protein in liver fibrosis. *Front Biosci (Landmark Ed)* 2019; 24(1): 1-17.
34. Fitzgerald AA, Weiner LM. The role of fibroblast activation protein in health and malignancy. *Cancer Metastasis Rev* 2020; 39(3): 783-803.
35. Zhou Y, Yang X, Liu H et al. Value of ^{68}Ga-FAPI-04 imaging in the diagnosis of renal fibrosis. *Eur J Nucl Med Mol Imaging* 2021; 48(11): 3493-501.
36. Djudjaj S, Boor P. Cellular and molecular mechanisms of kidney fibrosis. *Mol Aspects Med* 2019; 65: 16-36.
37. Fitzgerald AA, Weiner LM. The role of fibroblast activation protein in health and malignancy. *Cancer Metastasis Rev* 2020; 39(3): 783-803.
38. Chang WY, Tseng NC, Chen LY et al. Comparison of the Detection Performance Between FAP and ^{18}F-FDG PET/CT in Various Cancers: A Systemic Review and Meta-analysis. *Clin Nucl Med* 2023; 48(2): 132-42.
39. Cui Y, Wang Y, Wang S et al. Highlighting Fibroblasts Activation in Fibrosis: The State-of-The-Art Fibroblast Activation Protein Inhibitor PET Imaging in Cardiovascular Diseases. *J Clin Med* 2023; 12(18): 6033.